

CRACK PROPAGATION IN PRESTRESSED CONCRETE.
INTERACTION WITH REINFORCEMENT

S. Chhuy*, M.E. Benkirane*, J. Baron*, D. François**

*Laboratoire Central des Ponts et Chaussées
58, Bd Lefebvre - 75732 Paris Cedex 15

**Université de Technologie de Compiègne
B.P. 233 - 60206 Compiègne

ABSTRACT

The extend of the microcracked zone ahead of the main crack and the fracture energy of concrete were measured as a function of crack propagation in large DCB specimens prestressed to various levels. The fracture energy was found to evolve from an initiation value to a steadystate value which was the lower the larger the prestressing load. The crack interaction with two steel bars reinforcements across the crack path was found to be only slight.

KEY WORDS

Fracture toughness, concrete, reinforcement, prestressing.

INTRODUCTION

As only the parts in compression enter in the calculations of concrete structures, cracks are implicitly accepted. However they can sometimes by accident put a construction in danger. Fracture mechanics should then help to better estimate its behavior. Many authors thus attempted to measure the fracture toughness of concrete (all references are listed at the end) and the influence of various structural parameters on this characteristic. It appears that a large microcracked zone extends ahead of the main crack, making questionable the use of linear elastic fracture mechanics. For the tests to be valid the microcracked zone must remain imbedded within an elastic continuum. The quoted tests generally did not meet this condition and the reported toughnesses are therefore an increasing function of the specimen size (fig. 1). On the other hand the fracture energy is often considered as constant as the crack propagates, whereas the probable evolution of the microcracked zone should bring about a similar variation of the toughness. Lastly we are not aware of any study of the influence of reinforcement on the fracture energy.

The present study thus attempts to answer the preceding questions by choosing a specimen large enough for the confinement of the microcracked zone, and insuring the control of the crack growth. Tendons with various levels of prestressing were included in the test beams and in some cases passive reinforcements were added across the crack path.

CRACK PROPAGATION IN CONCRETE

Experimental Device

The crack propagation study was carried out on a large double cantilever beam specimen (DCB) with a narrower central section as shown on fig. 2. Longitudinal prestressing was introduced by several cables altogether loaded to 48, 106 or 212 tons.

Table I gives the experimental conditions of the various tests.

TABLE I Experimental Conditions

Test Number	Age (days)	Beam	Acoustic emission	Specimen length (m)	Prestress (tons)
DCB 2	70	no reinforcement	yes	2.50	48
DCB 6	28	no reinforcement	yes	3.50	106
DCB 7	28	reinforced	yes	3.50	106
DCB 10	28	no reinforcement	no	3.50	212
DCB 12	28	reinforced	yes	3.50	106

The beam was suspended vertically, the notch at the bottom, the crack propagating upwards. Electrical strain gages were glued along the axis of symmetry of the beam. Four extensometers allowed to measure the crack opening displacements at various locations. The applied load P was also deduced from the recording of the pressure in the hydraulic ram, and the crack length a was measured using a magnifying glass. The loading program was a succession of the following steps. The displacement V_1 was increased linearly as a function of time for 50 seconds at a velocity of $1 \mu\text{msec}^{-1}$. It was then held constant until the load P relaxed to a constant value. After the crack had propagated for a large enough length, the load was released before resuming the test. An acoustic emission device including two transducers at a distance of, 40 or, 70cm allowed to follow the extension of the microcracked zone at the head of the main crack.

Experimental Results

A recording of the load P versus the displacement V_1 is shown on the figure 3. The same kind of recording was obtained in all cases. The recordings of the displacements V_1 , V_2 , V_3 and V_4 as a function of time gave the evolution of the crack profile.

When the prestressing loads were larger than 48t. the unloading-reloading curves were not straight lines through the origin but loops as shown on figure 3. They can be approximated by two straight seq-

ments OI and IM which meets the ordinate axis at a load P_0 , a function of the crack length a .

Figure 4 shows this variation for a number of tests. It can be explained by the curvature of the beams due to the prestressing loads. The available energy rate for the crack to propagate from a to $a + da$ is measured by the area OIMM'JO \approx AMM'. As the compliance C of the beam is such as $V = C(P - P_0)$, the available energy rate G is given by

$$G = \frac{1}{2t} (P - P_0)^2 \frac{dC}{da}$$

where t is the thickness and the test piece behaved, as far as fracture is concerned, as if the applied load was $P - P_0$ and not P .

The microcracked zone was considered to include all points where the strain gages readings exceeded 10^{-4} . The length of this zone appeared to remain approximately constant as the main crack propagated. For instance it was 20 cm for a prestressing load of 106 t. The acoustic emission localisation showed an evolution of the microcracked zone at the beginning of the test, the acoustic events multiplying on a distance of about 15 cm. However a few events were recorded as far ahead of the crack tip as 50 cm (Chhuy, 1979)

For all prestressing loads used, the crack propagation energy (or the critical stress intensity factor K_{IC}) reached a constant value after the crack propagated on a distance of about 1m (fig. 5). The value K_{IC} corresponding to the first crack advance ($\Delta a = 0$) increased with the prestressing load (fig. 6) whereas, the value K_{IC} corresponding to the steady state propagation decreased as the prestressing load was increased. This fact suggests that at this stage of crack propagation, the prestressing load limits the size of the microcracked zone and favors unstable crack propagation. This instability was indeed noticed on tests where the prestressing load was larger than 106 t., when K_{IC} was larger than K_{IC} . The extrapolation of the plots of K_{IC} versus prestressing load yields $K_{IC0} = 1 \text{ MPa } \sqrt{\text{m}}$ and $K_{IC} = 6 \text{ MPa } \sqrt{\text{m}}$ for no prestressing.

CRACK PROPAGATION IN REINFORCED CONCRETE

Experimental Device

The experimental device is the same as the one described previously except that two steel bars $2 \text{ } \phi \text{ } 6 \text{ HA}$ are included at 139 cm from the notch across the crack path (fig. 2b). The use of only one steel bar was not possible due to the prestressing cables α' and α which lied in the plane of symmetry $x'x$ of the beam. Electrical strain gages were glued 10 cm apart on each steel bar.

Results

The steel bars reinforcements appeared not to affect the microcracked zone whose length remained equal to about 20 cm until the end of crack propagation.

The strain gages on the steel bars showed that they began to be loaded when the crack tip reached a distance of about 30 cm from the

bars. The strain gages gave the deformation ϵ of the bars. The active length ($\epsilon > 0$) was about 20 cm. It is to be noted that they remained elastic even once the crack tip had crossed over the bars. (The larger value of ϵ was recorded in DCB 12 as $2,7 \cdot 10^{-3}$ whereas the elastic limit is $4 \cdot 10^{-3}$).

As long as the crack tip was at a distance of the steel bars larger than 20 cm, they had no effect on the fracture energy (fig. 7). As the length of the microcracked zone did not change when crossing the steel bars, the slight increase of the fracture energy which could then be noticed, could be due to perturbations in the concrete next to the bars, followed by the closing force which they exerted on the crack. It is indeed possible by subtracting from the K factor due to the applied load, the K factor due to the steel bars, to almost suppress this increase of the fracture energy.

CONCLUSIONS

1. The fracture toughness of concrete evolves as the crack propagates. Its initial value is an increasing function of the prestressing load whereas it reaches a constant value the lower the larger this load. Larger than $1 \text{ MPa} \sqrt{\text{m}}$ in any case, the steady state fracture toughness reached $4 \text{ MPa} \sqrt{\text{m}}$ for the smallest prestressing load tested.

2. Steel bars reinforcements, which are loaded along a distance of about 20 cm when crossed by the crack, do not change the length of the microcracked zone and brings about only a slight increase of the fracture energy, mostly due to the closing force opposing the crack opening.

REFERENCES

Kesler, C.E., D.J. Naus and J.L. Lott (1972). Fracture mechanics- its applicability to concrete. Proceedings of the International conference on Mechanical Behavior of Materials (Japan), 4, 113 - 124.
 Walsh, P.F. (1972). Fracture of plain concrete. The Indian Concrete Journal, 46, 469-470-476.
 Entov, V.M. and V.I. Yagust (1975). Experimental investigation of Laws Governing Quasi-static development of macrocracks in concrete. IZV AN SSSR. Mekhanika Tverdogo Tela, 10, 93-103.
 Glücklich, J. (1963). Fracture of plain concrete. Journal of the Eng. Mechanics Division, 89, 127-138.
 Lott, J.L. and C.E. Kesler (1966). Crack propagation in plain concrete. Symposium on Structure of Portland Cement Paste and concrete (Washington), DC, Highway Research Board, 204-218.
 Baron, J. (1977). Comportement du béton hydraulique : Fissurabilité et fragilité. Etude bibliographique et critique. Rapport de recherche LPC n° 69.
 Chhuy, S., J. Baron and D. François (1979). Mécanique de la rupture appliquée au béton hydraulique, Cement and Concrete Research, 9, 641-648.

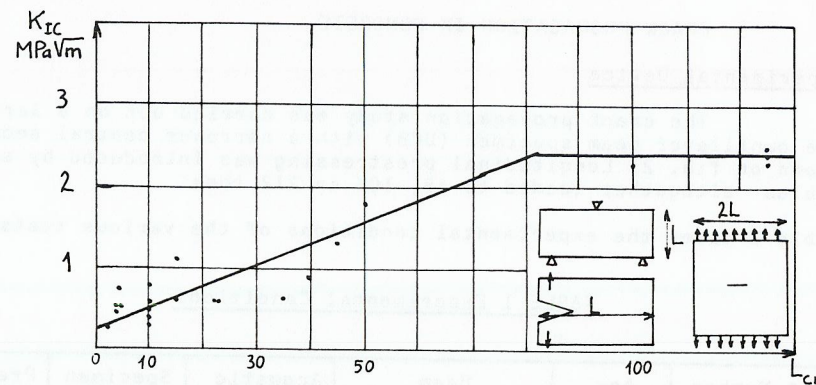


Fig. 1. Reported values of the fracture toughness of concrete versus the dimension of the specimen ligament (the references are in the text).

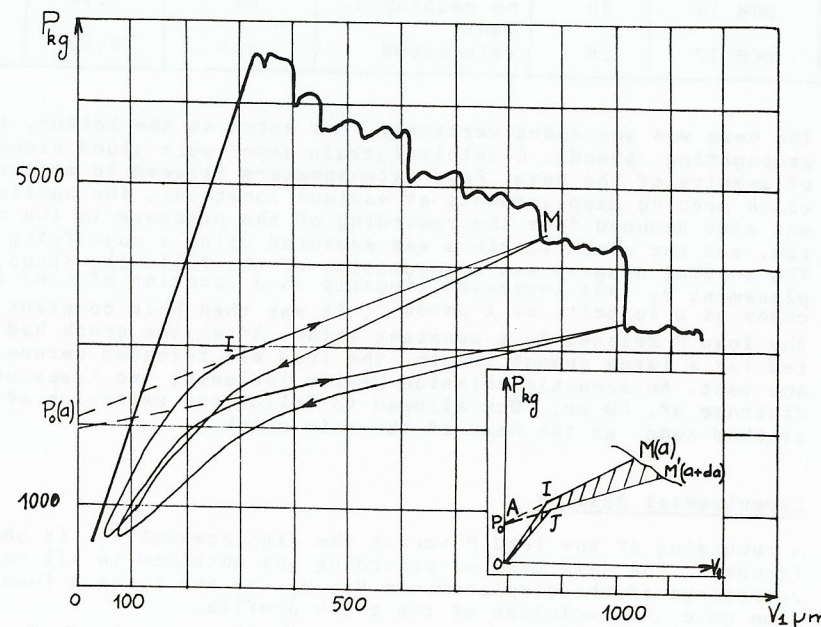


Fig. 3. Load versus displacement recording and unloading-reloading loops (DCB 12, prestressing load 106 t). The schematic drawing explains the way G was evaluated.

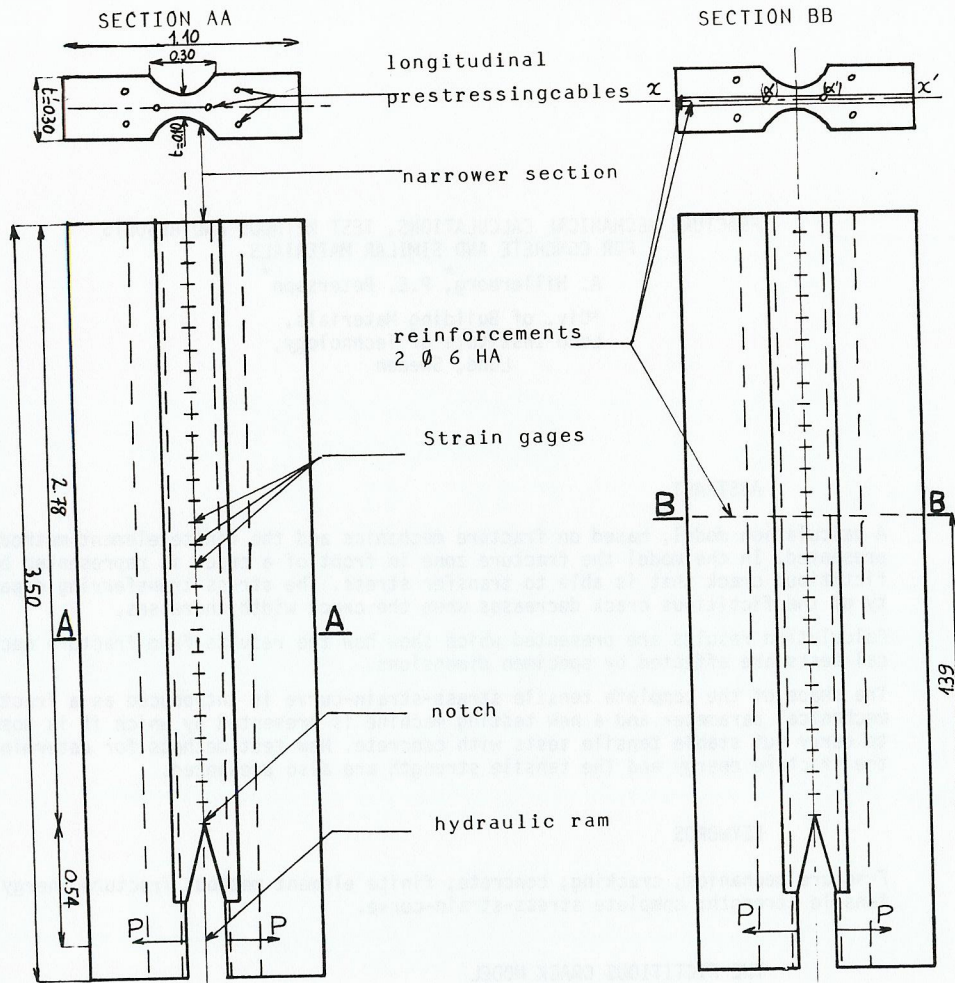


Fig. 2a

Fig. 2. Schematic drawing of the DCB specimen used (2a : without reinforcements, 2b : with reinforcements). The four extensometers are located at a distance of 0, 54, 84 and 193 cm from the hydraulic ram. They measure the displacements V_1, V_2, V_3 and V_4 . The composition of the concrete was for 1 m³ : cement : 400 kg (class CPA 400), sand : 700 kg, gravel : 1105 kg, water : 190 kg.

fig. 2b

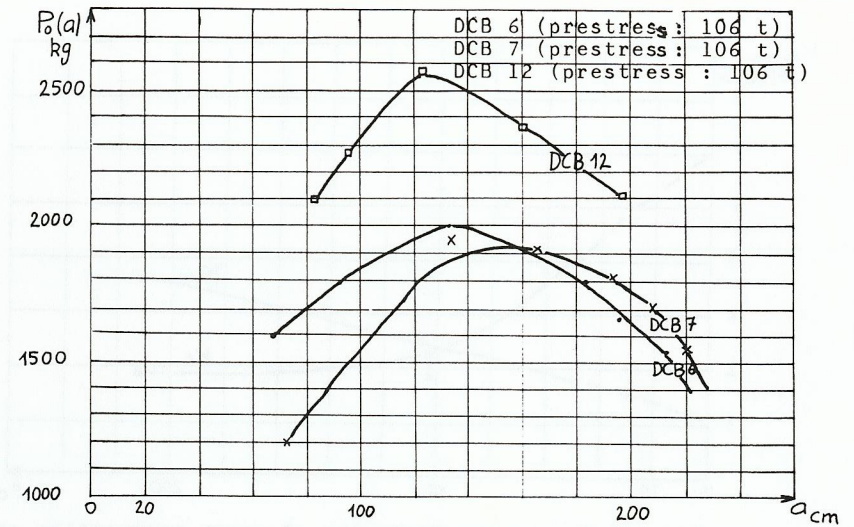


Fig. 4. Plot of the load P_0 (see Fig. 3) versus crack length a .

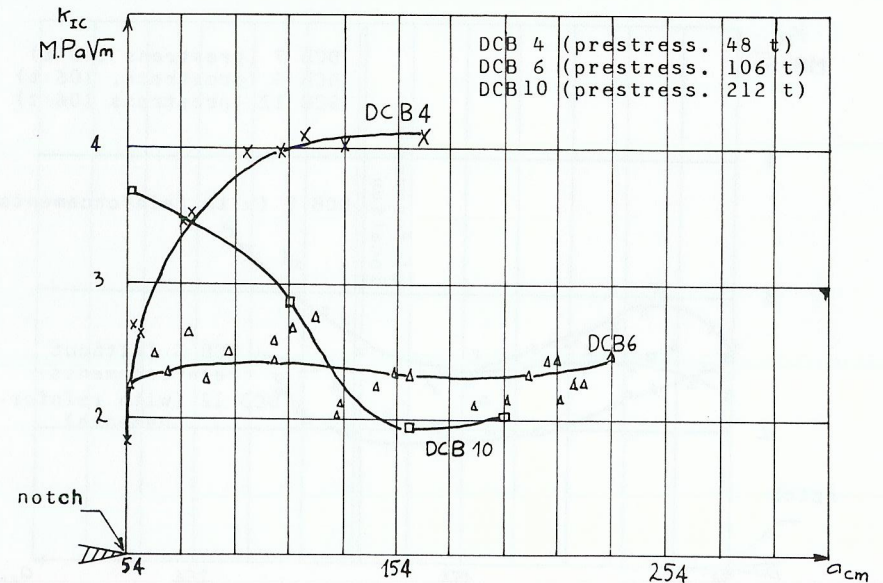


Fig. 5. Plot of the fracture toughness K_{Ic} versus the crack length a for various levels of prestressing load (no reinforcements).

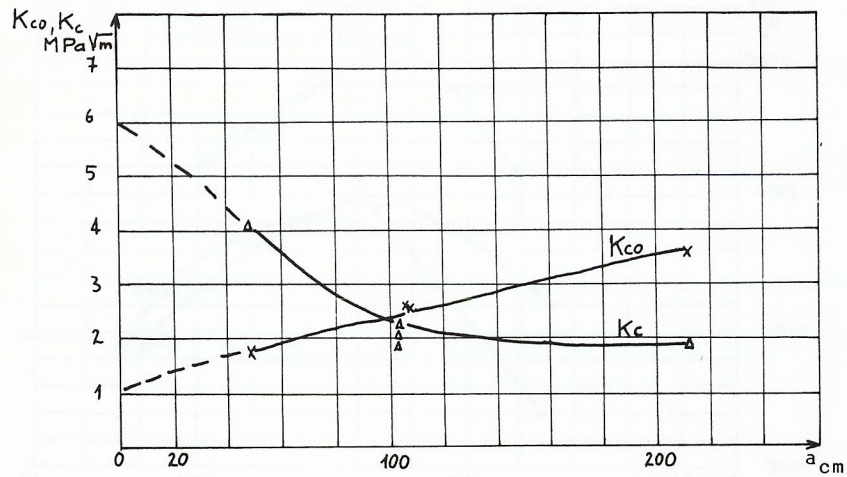


Fig. 6. Plot of K_{co} at the beginning of crack propagation and of K_c at steady state crack propagation versus the prestressing load.

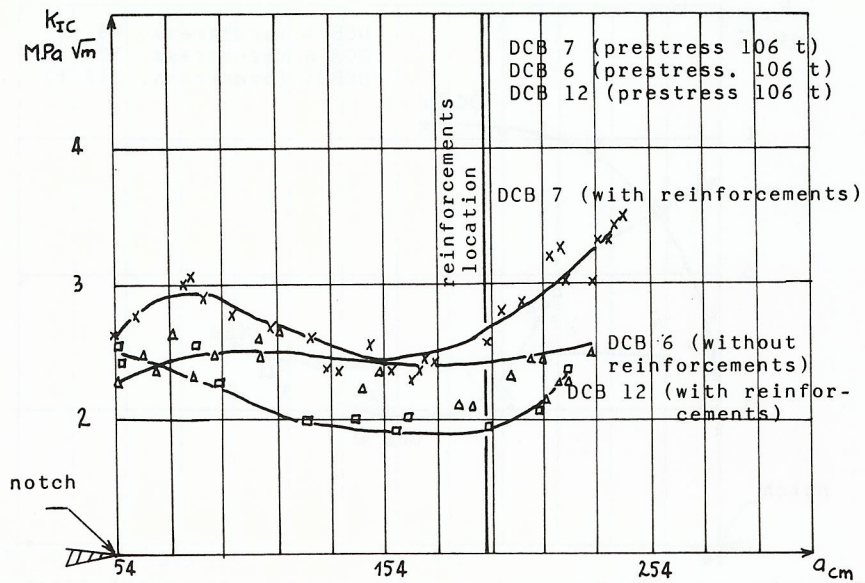


Fig. 7. Comparison of the evolution of the fracture toughness K_c versus the crack length a for concrete with and without reinforcements.